



**HAL**  
open science

## Elaboration of $\text{CaLa}_2\text{S}_4$ transparent ceramics from novel precursor powders route

Odile Merdrignac-Conanec, Guillaume Durand, Sebastian Walfort, Noha Hakmeh, Xianghua Zhang

► **To cite this version:**

Odile Merdrignac-Conanec, Guillaume Durand, Sebastian Walfort, Noha Hakmeh, Xianghua Zhang. Elaboration of  $\text{CaLa}_2\text{S}_4$  transparent ceramics from novel precursor powders route. *Ceramics International*, 2017, 43 (8), pp.5984-5989. 10.1016/j.ceramint.2017.01.132 . hal-01458361

**HAL Id: hal-01458361**

**<https://hal.science/hal-01458361>**

Submitted on 10 Feb 2017

**HAL** is a multi-disciplinary open access archive for the deposit and dissemination of scientific research documents, whether they are published or not. The documents may come from teaching and research institutions in France or abroad, or from public or private research centers.

L'archive ouverte pluridisciplinaire **HAL**, est destinée au dépôt et à la diffusion de documents scientifiques de niveau recherche, publiés ou non, émanant des établissements d'enseignement et de recherche français ou étrangers, des laboratoires publics ou privés.

Elaboration of  $\text{CaLa}_2\text{S}_4$  transparent ceramics from novel precursor powders route

Odile Merdrignac-Conanec\*, Guillaume Durand, Sebastian Walfort, Noha Hakmeh,  
Xianghua Zhang

Institut des Sciences Chimiques de Rennes, UMR CNRS 6226, Equipe Verres et  
Céramiques, Université de Rennes1, Campus de Beaulieu, 35042 Rennes Cedex, France

\*Corresponding author: Dr. Odile Merdrignac-Conanec Institut des Sciences Chimiques  
de Rennes, UMR CNRS 6226, Equipe Verres et Céramiques Université de Rennes 1,  
Campus de Beaulieu, 35042 Rennes Cedex, France. Phone : +33 (0)2 23 23 62 66; Fax :  
+33 (0)2 23 23 56 11@fax.univ-rennes1.fr. Email : odile.merdrignac@univ-rennes1.fr

#### Abstract

A cost-effective processing route for the production of calcium lanthanum sulfide  $\text{CaLa}_2\text{S}_4$  (CLS) via a novel fast fabrication of precursor powders is reported. The sinterability of the newly developed powders was investigated by use of Hot-Pressing and pressureless sintering. Complementary techniques (XRD, SEM-EDS, chemical analysis, SSA, FT-IR spectroscopy) were employed to correlate the sintering processes and parameters to the microstructural/compositional developments and optical performances of the densified ceramics. Dense (>99.8% theor.) and homogeneous CLS ceramics were produced by pressureless sintering at 1250°C for 12 h in  $\text{H}_2\text{S}$  followed by hot-pressing at 1000°C for 6 h in a powder bed to prevent sulfur loss. Transparency free of impurity absorption has been achieved in the LWIR region (optical transmission of 51% in the 12-14  $\mu\text{m}$  range).

*Keywords* : D. calcium lanthanum sulfide; A. combustion synthesis; A. sintering; E. transparent ceramic

#### 1. Introduction

The development of infrared-transmitting materials started in the mid 1950s as a response to the growing demand for military and commercial instruments with improved optical and mechanical properties. Especially the newly invented "heat-seeking" missile required a more durable infrared-transmitting protective dome [1]. Zinc sulfide (ZnS) is the most suitable of the present infrared window materials especially for its performance at elevated temperature [2]. However, ZnS optics, currently available at a relatively high cost as chemical-vapour-deposited (CVD) polycrystalline materials, have poor resistance to erosion by rain and sand or dust particles and require durable protective coatings for external use [3]. In the early 1980s, compounds of the  $\text{CaLa}_2\text{S}_4$ - $\text{La}_2\text{S}_3$  solid solution system (CLS) emerged as alternative window materials to CVD ZnS, mainly based on their superior mechanical properties, better erosion resistance and longer transmission in the long wave infrared (LWIR) window up to 14  $\mu\text{m}$  [4-11]. A higher domain of transparency in the infrared significantly improves the performance of the infrared optical systems and allows the use of uncooled detectors (operate beyond 12  $\mu\text{m}$ ), resulting in a significant reduction in system cost. Two chemical routes (Evaporative Decomposition of Solution and precipitation) were proposed for the preparation of the precursor powder [11-14] but the development of the ceramics never arrives to commercial maturity. Indeed, the reproducibility of the optical properties of the sintered materials remained a problem which was thought to be a result of variability of the powder [11] caused or increased by lengthy and complicated processes. For both methods, the sole sulfurization step of the precursors required times up to several days.

The present work reports the development of CLS infrared window materials, using an innovative energy-saving wet-route synthesis process. In the literature, the material

referred to is not necessarily the stoichiometric compound  $\text{CaLa}_2\text{S}_4$  with  $\text{La}/\text{Ca} = 2$ , but a material with a higher  $\text{La}/\text{Ca}$  ratio most prominently  $\text{La}/\text{Ca} = 2.7$  [8,11]. The  $\text{La}/\text{Ca}$  ratio is adjustable because  $\text{CaLa}_2\text{S}_4$  forms a complete solid solution with the isostructural cubic lanthanum sesquisulfide  $\gamma\text{-La}_2\text{S}_3$ . In fact, the study of CLS basically originated from the processing difficulties that existed for synthesizing the cubic  $\gamma\text{-La}_2\text{S}_3$ , which forms at temperatures in excess of  $1300^\circ\text{C}$ . It was found [15-17] that the addition of large divalent cations, namely  $\text{Ca}^{2+}$ , could stabilize the cubic structure at much lower temperatures. There is, therefore, a continuous and homogeneous range of stoichiometries for the ternary  $\text{Ca}_x\text{La}_{(8-2x)/3}\square_{(1-x)/3}\text{S}_4$  where  $\square$  represents a vacancy ( $x \in [0,1]$ ) [15]. CLS can alternately be described as a Ca doped  $\gamma\text{-La}_2\text{S}_3$  and denoted as  $\gamma\text{-La}_2\text{S}_3:\text{Ca}$ .

In order to investigate the efficiency of the novel precursor synthesis, various Ca amounts ( $\text{La}/\text{Ca} = 2.7, 5$  and  $9$ ) were employed to evaluate the effects and abilities of  $\text{Ca}^{2+}$  cation to stabilize the cubic  $\gamma\text{-La}_2\text{S}_3$ . We investigated, next, the densification of the newly developed powders to produce transparent ceramics. The study explored the influences of sintering conditions (temperature, time, pressure) on the microstructure and optical properties of the ceramics and discussed the conditions for producing LWIR transparency free of impurity absorption.

## 2. Experimental procedure

### 2.1. Precursor powders and ceramics processing

CLS powders were prepared by a novel patented solution combustion method followed by a sulfurization step [18]. Lanthanum nitrate hexahydrate  $\text{La}(\text{NO}_3)_3 \cdot 6\text{H}_2\text{O}$  (Alfa Aesar, 99,99%), calcium nitrate hydrate  $\text{Ca}(\text{NO}_3)_2 \cdot 4\text{H}_2\text{O}$  (Alfa Aesar, 99,98%) and thioacetamide (TAA)  $\text{CH}_3\text{CSNH}_2$  (Sigma Aldrich,  $\geq 99\%$ , ACS Reagent) were used

as starting materials. Different preparations with  $\text{La}/\text{Ca}$  molar ratios of  $2.7, 5$  and  $9$  were investigated. As-combusted powders were subsequently heat-treated under pure  $\text{H}_2\text{S}$  flow in a tubular furnace at  $1000^\circ\text{C}$ .

Next, pure CLS powders were either hot-pressed directly into ceramic pellets or hot-pressed after pressureless pre-sintering in  $\text{H}_2\text{S}$  at  $1250^\circ\text{C}$  for 12 h. The pre-sintered samples were placed in a bed of CLS or boron nitride BN (Alfa Aesar 99,5%) powders during hot-pressing. Hot pressing was carried out under dynamic vacuum (about  $10^{-2}$  mbar). Powdered samples or pre-sintered samples were directly heated to the sintering temperature from room temperature at a heating rate of  $10^\circ\text{C}/\text{min}$ . A typical quantity of  $3.5$  g (or  $2$  g) of powder was introduced in a  $20$  mm (or  $13$  mm) diameter graphite mould coated beforehand with BN to prevent carbon diffusion and facilitate demoulding.  $50$  MPa and  $120$  MPa were applied at selected sintering temperatures ( $950^\circ\text{C}$  to  $1150^\circ\text{C}$ ) for different dwell times (1h to 6h). Some samples were re-sulfurized in  $\text{H}_2\text{S}$  at  $1000^\circ\text{C}$  for 3 hours, after hot-pressing.

### 2.2. Characterisation

X-ray diffraction (XRD) patterns were recorded at room temperature in the  $2\theta$  range  $5\text{-}90^\circ$  with a step size of  $0.026^\circ$  and a scan time per step of 40s using a PANalytical X'Pert Pro diffractometer (Cu  $K\alpha$  radiation,  $\lambda = 1.5418\text{\AA}$ , PIXcel 1D detector). Data Collector and High-Score Plus softwares were used, respectively, for recording and analysis of the patterns. The ceramic XRD patterns for Rietveld refinements were recorded at room temperature in the  $2\theta$  range  $5\text{-}120^\circ$  with a step size of  $0.026^\circ$  and a scan time per step of 400s. All calculations were carried out with Fullprof program [19].

Oxygen contents were determined with a Leco<sup>®</sup> TC-600 analyzer using the inert gas fusion method in which oxygen was measured as  $\text{CO}_2$  by infrared detection. A

FlowSorb II 2300 Micromeritics apparatus was used to determine the specific surface area (SSA) of the powders by the Brunauer-Emmett-Teller single point method. Before measurement, the samples were outgassed under N<sub>2</sub>/He flow at 250°C for 30 min.

Densities of the sintered samples were measured in pure ethanol according to Archimedes' principle.

The morphology and microstructure of the CLS powders and polished surfaces of the ceramics samples were examined by Scanning Electron Microscopy (SEM) using JEOL JSM 6301 equipment. The insulating samples were metallized with Au-Pd. The composition of the samples was analyzed by Energy Dispersive Spectroscopy (EDS), attached to the SEM.

Fourier Transform Infrared (FT-IR) spectroscopy was carried out with a Nicolet 380 FT-IR spectrometer (Thermo Electron Corporation) in the 400-4000 cm<sup>-1</sup> range. Sintered samples were simply placed in the beam line, while powders were pressed into pellets, after careful grinding with anhydrous KBr (99+%, FT-IR grade, Sigma-Aldrich). FT-IR spectra of powders were recorded by reference to a freshly prepared blank KBr pellet. Infrared transmission spectra of the ceramics specimens were performed using the same equipment in the 2-16 μm range.

### 3. Results

#### 3.1. Precursor powders

For the three starting mixtures investigated (La/Ca = 2.7, 5 and 9), XRD characterisation identifies lanthanum oxysulfate La<sub>2</sub>O<sub>2</sub>SO<sub>4</sub> and lanthanum oxide La<sub>2</sub>O<sub>3</sub> as major phases in the raw (as-combusted) powders with small amounts of lanthanum oxysulfide La<sub>2</sub>O<sub>2</sub>S. After treatment in pure H<sub>2</sub>S flow at 1000°C for 4 h, pure cubic CLS phase is obtained for raw powders with La/Ca = 2.7 whereas for higher molar ratios

(La/Ca = 5, 9), β-La<sub>2</sub>S<sub>3</sub> was detected as an additional phase due to a less efficient stabilization of the CLS cubic phase by lower Ca contents (Fig.1).

Total conversion into CLS therefore requires, for these ratios, longer heat treatments and/or treatments at higher temperatures which also lead to particles growth that is detrimental to the powder sinterability. To favour short-term treatment at moderately low temperature, powder synthesis experiments were performed with the ratio La/Ca = 2.7. All the ceramics further investigated in this study were elaborated from CLS powders with the initial La/Ca ratio of 2.7.

Representative FTIR transmission spectra obtained from the powders before and after sulfurization under H<sub>2</sub>S are shown in Fig. 2. Spectra of the as-combusted powders show strong absorption bands at 3300-3700 cm<sup>-1</sup> and 1630 cm<sup>-1</sup>, that are characteristic of ν<sub>3</sub> asymmetric and ν<sub>1</sub> symmetric stretching and bending modes of the H<sub>2</sub>O molecule [20-22]. The stretching vibrations of sulfate groups, observed at 560-700 cm<sup>-1</sup> and 1000-1250 cm<sup>-1</sup>, are attributed to the S-O vibration bands of La<sub>2</sub>O<sub>2</sub>SO<sub>4</sub> and La<sub>2</sub>O<sub>2</sub>S previously identified by XRD [23]. Finally, a large band can be observed around 1350-1580 cm<sup>-1</sup> due to carbonate species [24, 25]. This absorption band originates from the presence on the surface of the particles of adsorbed CO<sub>2</sub> from the air and/or combustion reaction. All the characteristic O-H, S-O and C-O absorption bands observed in the as-combusted powders are removed after sulfurization. Heat treatment of raw powders under pure H<sub>2</sub>S at 1000°C for 4 h has thus proven to be an effective process to produce high purity CLS powders.

SEM images of raw and H<sub>2</sub>S heat-treated powders are presented in Fig. 3. It can be observed that the raw powder (Fig. 3a) shows submicronic (100-400 nm) flaky particles that form large agglomerates. The sulfurization treatment considerably alters the size and the morphology of the individual particles (Fig. 3b). The particle size itself

increases to about 500 nm and the shape becomes much more rounded. In addition, the formerly individual particles partially sinter and form big porous structures.

### 3.2. Ceramics

#### 3.2.1. Density and Visual Aspect

Table 1 reports the sintering parameters and the density of the hot-pressed (HPed) ceramics. The sintered densities of all the samples were measured according to Archimedes' principle. The theoretical density of CLS (La/Ca=2.7) was determined from XRD characterisation assuming a linear interpolation between the known lattice constants of the stoichiometric compounds  $\text{CaLa}_2\text{S}_4$  ( $a=8.683 \text{ \AA}$ ,  $\rho=4.53 \text{ g.cm}^{-3}$ ) and  $\gamma\text{-La}_2\text{S}_3$  ( $a=8.731 \text{ \AA}$ ,  $\rho=4.98 \text{ g.cm}^{-3}$ ) and calculation from the general formula of the binary solid solution  $\text{Ca}_x\text{La}_{(8-2x)/3}\square_{(1-x)/3}\text{S}_4$  [13,15]. The theoretical density of CLS with La/Ca=2.7 is calculated to be  $4.62 \text{ g.cm}^{-3}$ .

Table 1 Sintering parameters and densities of HPed samples.

Sample	CLS1	CLS2	CLS3*	CLS4	CLS5	CLS6**	CLS7**
T (°C)	950	1100	1150	1000	1000	1000	1000
Dwell time (h)	3	1	2	2	6	6	6
Pressure (MPa)	50	50	50	120	120	120	120
Density (% theor.)	98.0	99.6	99.4	98.5	99.1	99.8	99.8

\* Sample re-sulfurized in  $\text{H}_2\text{S}$  at  $1000^\circ\text{C}$  for 3 h after HP

\*\* Pre-sintered sample in  $\text{H}_2\text{S}$  at  $1250^\circ\text{C}$  for 12 h before HP

Photographs of CLS1, CLS2, CLS3, CLS5 and CLS7 ceramic samples sintered between  $950^\circ\text{C}$  and  $1150^\circ\text{C}$  are presented in Fig. 4. Samples sintered at  $950^\circ\text{C}$  (CLS1) remain primarily yellow, similar to the sulfurized precursor powder. With increasing

sintering temperatures (samples sintered at intermediate temperatures of  $1000^\circ\text{C}$  and  $1050^\circ\text{C}$ , not presented here), ceramics appear progressively darker and this becomes more pronounced from  $1100^\circ\text{C}$  (CLS2). The colour can be restored to a homogeneous yellow by re-sulfurization (CLS3). Finally, CLS5 and CLS7 samples HPed at moderate temperature ( $1000^\circ\text{C}$ ) exhibit a brownish colouration which could originate from longer sintering time (6 h) and/or higher load pressure (120 MPa). It must be mentioned here that pre-sintered samples obtained after a pressureless sintering in  $\text{H}_2\text{S}$  at  $1250^\circ\text{C}$  for 12 h retained their initial yellow colour. Density results will be discussed in section 4.

#### 3.2.2. XRD characterisation

Fig. 5 presents the typical XRD pattern of the series CLS1-CLS5 samples and the patterns of CLS6 and CLS7 pre-sintered samples before and after hot-pressing. No drastic change is observed in the CLS1-CLS5 ceramics patterns compared to the precursor powders except the appearance of a small amount of  $\beta\text{-La}_2\text{S}_3$  as second phase. In contrast, CLS6 and CLS7 pre-sintered samples remained pure CLS compounds after hot-pressing.

#### 3.2.3. Transmission spectra

Five specimen (CLS3, CLS4, CLS5, CLS6 and CLS7) showed transmission in the desired wavelength range (Fig. 6). With a maximum density of 98%, CLS1 sample remained opaque. Despite a good densification (99.6%), the transmission of CLS2 sample is essentially zero. From its visual aspect, we assume this sample to have experienced some severe reduction during HP. The dark grey sample CLS3, initially HPed at  $1150^\circ\text{C}$  for 2 hours under 50 MPa, was re-sulfurized and re-polished. Upon re-

sulfurization, the 1.4 mm thick sample offers a transmission percentage up to 14% at 13  $\mu\text{m}$ . These results are further addressed in section 4.

In contrast, samples sintered by application of 120 MPa at 1000°C all turned transparent. However, all transmission spectra of samples issued from direct HP present absorption bands located around 9  $\mu\text{m}$  and 11  $\mu\text{m}$  in Fig. 6. The intense absorption band at 11  $\mu\text{m}$  is attributed to sulfate species ( $\text{SO}_3^{2-}$ ) which might be caused by adsorbed oxygen on the surface of powders when exposed to air [26]. The small  $\text{SO}_4^{2-}$  band at about 9  $\mu\text{m}$  originates from oxygen traces stabilizing the  $\beta\text{-La}_2\text{S}_3$  ( $\text{La}_{10}\text{S}_{14}\text{O}$ ) [27]. This result is in agreement with the XRD characterisation which identified  $\beta\text{-La}_2\text{S}_3$  as second phase. The best performance, in the strategic 10-14  $\mu\text{m}$  range, related to transmission level and occurrence of sulfate bands is observed with pre-sintered samples.

#### 4. Discussion

##### 4.1. Combustion synthesis and sulfurization

The solution combustion synthesis is a fast and expeditious process. The entire reaction appears to be over after only a few minutes. It produces bright white foamy agglomerates that are easily crushed into a powder with a mortar and pestle. During the sulfurization process, the colour changes throughout the entire batch to the expected pale yellow colour of CLS and complete reaction in about 4 h. A further change in the powder colour with sulfurization time is not observable with the naked eye. The submicron size and the plate-like shape of the primary particles allow short diffusion paths for sulfur and subsequently fast sulfurization process. This method thus raised considerable interest for time saving and economical consideration, compared to the more conventional methods reported in the introduction.

##### 4.2. Densification of the CLS powders

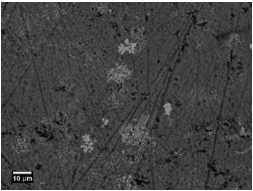
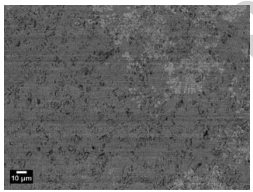
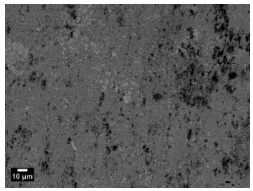
The present synthesis procedure, which involves heat treatment at elevated temperature, produces powders partially sintered, as observed from the SEM. Their sinterability remains however consistent with enabling near theoretical densification. Densification to >99% of theoretical density is reached at moderate temperature (1000°C) and applied load of 120 MPa. For a pressure of 50 MPa, however, it appears as if the maximum densification attained is 98% which is inferior to the transparency threshold and increasing sintering temperatures do not necessarily lead to higher densities. The density of sample sintered at 1150°C for 2 hours was indeed lower than that of the sample sintered at 1100°C for 1 hour. The high differences in visual appearance and density between samples sintered at temperatures only 100-150°C apart can be explained by the sudden increase in vapour pressure within the relevant temperature range. This change in visual aspect becomes significant at 1150°C and suggests a shift of the composition towards sulfur-deficient phases, this critical point is discussed in section 4.3. Based on a simplified Antoine equation, Nikolaev *et al.* proposed an analytical equation for the saturated vapour pressure as a function of temperature for  $\text{La}_2\text{S}_3$  [28]. It shows that the vapour pressure quickly rises in the (relevant, in this work) temperature range from 900°C to 1200°C. It is also reported that even very slight deviations in the stoichiometry from  $\text{La}_2\text{S}_3$  towards the sulfur-deficient  $\text{La}_3\text{S}_4$  lead to a more metallic behaviour [29]. Sulfur volatilization severely inhibits densification and probably further reduces the transmission in the entire wavelength region due to free carrier absorption. Re-sulfurization in  $\text{H}_2\text{S}$  at 1000°C for 3 h (CLS3 sample) by restoring sulfur stoichiometry did improve the IR transmission. Results here are in agreement with an earlier report by Li *et al* [30] on  $\gamma\text{-La}_2\text{S}_3\text{:Ca}$  translucent ceramics elaborated by a different precursor route.

## 4.3. Correlation between sintering processes and parameters,

microstructural/compositional developments and optical properties

The compositions of the phases present in representative samples of the CLS1-CLS5 series were determined via SEM-EDS. Backscattered SEM (BSE-SEM) images of the analyzed areas clearly reveal the presence of a secondary phase (brighter contrast) (Table 2). The black spots in the images are due to porosity and the scratches arise from the coarse polishing. EDS analysis shows that the two phases present deviating compositions.

Table 2. Back scattered scanning electron micrographs (BSE-SEM) and EDS analysis obtained from polished surfaces of CLS2, CLS3 and CLS5 samples processed from direct HP.

Sample	Composition (atom%)	SEM-EDS		XRD refinement
		Phase 1	Phase 2	
 CLS2	Ca	12.3	1.5	13.4
	La	29.7	39.8	29.3
	S	58.0	58.7	57.3
	La/Ca	2.4		2.2
	S/La	2.0	1.5	2.0
 CLS3	Ca	12.2	1.6	12.3
	La	29.2	39.0	30.2
	S	58.6	58.7	57.5
	La/Ca	2.4		2.5
	S/La	2.0	1.5	1.9
 CLS5	Ca	12.6	0.0	13.5
	La	30.9	42.9	29.2
	S	56.5	57.1	57.3
	La/Ca	2.5		2.2
	S/La	1.8	1.3	2.0

The majority grey phase (phase 1) has an average composition of  $\text{Ca}_{0.12}\text{La}_{0.30}\text{S}_{0.58}$  lying on the  $\text{CaLa}_2\text{S}_4\text{-La}_2\text{S}_3$  join, with La/Ca and S/La ratios close, considering the accuracy of the EDS measurement, to the expected values of 2.7 and 2 respectively. The brighter phase (phase 2) has very little calcium and a S/La ratio varying from 1.5 to 1.3. EDS analysis correlates well with the XRD patterns measured on these samples which identify CLS as major phase and the sulfur-depleted phase  $\beta\text{-La}_2\text{S}_3$  (S/La=1.5) as second phase. As reported above,  $\beta\text{-La}_2\text{S}_3$  is responsible for the small  $\text{SO}_4^{2-}$  band at about 9  $\mu\text{m}$  in the transmission spectra and, additionally, with its tetragonal structure, could create birefringence and scattering in the samples. Note that the ratio S/La in CLS5 corresponds to that of cubic  $\gamma\text{-La}_3\text{S}_4$  (1.3); so we can not exclude the formation of small amounts of  $\text{La}_3\text{S}_4$  which could not be identified by XRD analysis (Fig. 5). CLS and  $\text{La}_3\text{S}_4$  are indeed isostructural with very similar lattice constants differing by only 0.5% [31]. In addition, we can mention that the chemical composition obtained after Rietveld refinements of the ceramic XRD patterns matches well that obtained by EDS analysis.

As expected from its low density (98.5%), CLS4 sample processed by direct HP at 120 MPa for 2 h exhibit a maximum transmission of only 25% at 13  $\mu\text{m}$ . By increasing the dwell time to 6 h (CLS5), densification to >99% is reached and the transmission is significantly improved (37% at 13  $\mu\text{m}$ ).

Overall the best results were obtained for CLS6 and CLS7 samples, pre-sintered (to about 94% densification) at 1250°C for 12 h in pure  $\text{H}_2\text{S}$ . CLS6 and CLS7 pre-sintered samples were placed in CLS and BN powders beds respectively and hot-pressed at 1000°C under 120 MPa. By contrast to the CLS1-CLS5 series, EDS analysis of CLS6 (S/La=2 and La/Ca=2.4) and CLS7 (S/La=2 and La/Ca=2.4) samples did not detect any secondary phase and revealed by X-ray elemental mapping a homogeneous composition

throughout the microstructure. Again, EDS results confirm the XRD analysis which did not identify  $\beta$ -La<sub>2</sub>S<sub>3</sub> as secondary phase. Pre-sintering in pure H<sub>2</sub>S for 12 h at 1250°C retains sulfur stoichiometry and helps remove residual oxygen thus prevents both the formation of  $\beta$ -La<sub>2</sub>S<sub>3</sub> (and possibly La<sub>3</sub>S<sub>4</sub>) and the occurrence of sulfate impurity absorption in the IR transmission spectra. Furthermore, pre-sintering at high temperature is beneficial to oxygen contamination also as a consequence of surface area reduction. Oxygen content in the CLS1-CLS5 series and specific surface area (SSA) of their precursor powders were respectively 0.35 wt.% and 1.1 m<sup>2</sup>.g<sup>-1</sup> while in CLS7 sample, these values were reduced to 0.025 wt.% and 0.3 m<sup>2</sup>.g<sup>-1</sup> respectively.

As a result, the optical transmissions obtained from these pre-sintered samples surpass those obtained on ceramics processed from direct HP. The best performance is observed in CLS7 sample with a maximum transmission reaching 51% in the 12-14  $\mu$ m range (theoretical transmission is 70% [29]). It is most likely that the sulfate band observed in CLS6 spectrum results from adsorbed oxygen, contained in the CLS powder (0.4 wt. %) used as sintering bed (no high temperature treatment in H<sub>2</sub>S prior to hot-pressing).

## 5. Conclusion

CLS transparent ceramics were successfully elaborated using a novel precursor powder route. The solution combustion synthesis developed in this work is an innovative fast (thus energy-saving) fabrication process of precursor powders. The latter are reproducibly sulfurized in a short time (4 h) compared to conventional methods (times up to several days). The newly developed powders can successfully produce infra-red transparent ceramics using hot-pressing and pressureless sintering. Powders, consequently ceramic optical quality, are extremely sensitive to processing conditions.

We showed that CLS compounds are very susceptible to oxygen contamination and stoichiometry deviation especially when subjected to direct hot-pressing in vacuum (sulfur loss).

Optimised sintering parameters thus consisted in pressureless sintering at 1250°C for 12 h in H<sub>2</sub>S followed by hot-pressing in a BN powder bed at 1000°C for 6 h. This process helps retain the initial chemical composition of the powder which is the main issue ever encountered in this complex solid solution system. Optical transmission of 51% in the 12-14  $\mu$ m range has been achieved with a ceramic densified to 99.8%. Future work will investigate the conditions for full densification completion and improvement of the optical performances at low wavelengths using longer HP treatment or Hot Isostatic Pressing (HIP) as post-sintering operation.

## Acknowledgements

This work was supported by the French Direction Générale de l'Armement and the industrial partner, Solcera Advanced Materials, Evreux, France.

## References

- [1] D.C. Harris, Development of hot-pressed and chemical-vapor-deposited zinc sulfide and zinc selenide in the united states for optical windows, Proc. SPIE Vol. 6545 (2007) 654-502.
- [2] J.A. Savage, K.L. Lewis, Fabrication of infrared optical ceramics in the CaLa<sub>2</sub>S<sub>4</sub>-La<sub>2</sub>S<sub>3</sub> solid solution system, Proc. SPIE Vol. 683 (1986) 79-84.
- [3] D.C. Harris, Materials for infrared windows and domes, Properties and Performance, SPIE Press (1999) p.60.



- [4] W.B. White, D. Chess, C.A. Chess and J.V. Biggers, CaLa<sub>2</sub>S<sub>4</sub>: Ceramic window material for the 8 to 14 μm region., Proc. SPIE 0297, Emerging Optical Materials (1982) 38-43 doi:10.1117/12.932482.
- [5] D.L. Chess, C.A. Chess, J.V. Biggers and W.B. White, Processing ternary sulfide ceramics: powder preparation, sintering, and hot-pressing, J. Am. Ceram. Soc. 66 (1) (1983) 18-22.
- [6] D.W. Roy, Progress in the development of ternary sulfides for use from 8 to 14 μm, Proc. SPIE 0297 Emerging Optical Materials (1982) 24-34 doi:10.1117/12.932480.
- [7] K.L. Lewis, J.A. Savage, K.J. Marsh and A.P.C. Jones, Recent developments in the fabrication of rare-earth chalcogenide materials for infrared optical applications, Proceedings of the Society of Photo-Optical Instrumentation Engineers 400 (1983) 21-28.
- [8] K.J. Saunders, T.Y. Wong, T.M. Hartnett, R.W. Tustison and R.L. Gentilman, Current and future development of calcium lanthanum sulfide, Proc. SPIE Vol. 683, Infrared and optical transmitting materials (1986) 72-78.
- [9] D.C. Harris, M.E. Hills, R.L. Gentilman, K.J. Saunders and T.Y. Wong, Fabrication and ESR characterization of transparent CaLa<sub>2</sub>S<sub>4</sub>, Adv. Ceram. Mater. 2(1) (1987) 74-78.
- [10] J.A. Beswick, D.J. Pedder, J.C. Lewis and F.W. Ainger, New infra-red window materials, New optical materials, Proc. SPIE 0400 New optical materials (1983) 12-20 doi:10.1117/12.935470.
- [11] M.E. Hills, Preparation, Properties, and Development of Calcium Lanthanum Sulfide as an 8- to 12-μm Transmitting Ceramic, Technical Report from the Naval Weapons Center, DTIC Document, China lake, CA (USA) (1989).

- [12] D.L. Chess, C.A. Chess and W.B. White, Precursor powders for sulfide ceramics prepared by evaporative decomposition of solutions, J. Amer. Ceram. Soc. 66 (11) (1983) C205-C207.
- [13] D.L. Chess, C.A. Chess, J.A. Marks and W.B. White, Phase equilibria and processing of infrared optical ceramics on the join CaLa<sub>2</sub>S<sub>4</sub>-La<sub>2</sub>S<sub>3</sub>, J. Ceram. Process. Res. 11(4) (2010) 465-470.
- [14] Raytheon Co., Development of calcium lanthanum sulfide as an optical ceramic, Lexington, Mass., Raytheon. (Annual Technical Report) (1987-1988).
- [15] J. Flahaut, L. Domange, M. Patrie, Combinaisons formées par les sulfures des éléments du groupe des terres rares. Etude cristallographique des phases ayant le type structural du phosphore de thorium Th<sub>3</sub>P<sub>4</sub>, Bull. Soc. Chim. Fr, 11-12 (1962) 2048-2054.
- [16] S.M. Golabi, J. Flahaut, L. Domange, Combinaisons de Type Th<sub>3</sub>P<sub>4</sub> formées entre les séléniures des terres rares et les séléniures alcalino-terreux, CR Acad. Sci. Paris, 259 (1964) 820-822.
- [17] J. Flahaut, M. Guittard, M. Patrie, M.P. Pardo, S.M. Golabi, L. Domange, Phase cubiques type Th<sub>3</sub>P<sub>4</sub> dans les sulfures, les séléniures et les tellurures L<sub>2</sub>X<sub>3</sub> et L<sub>3</sub>X<sub>4</sub> des terres rares, et dans leurs combinaisons ML<sub>2</sub>X<sub>4</sub> avec les sulfures et séléniures MX de calcium, strontium et baryum. Formation et propriétés cristallines, Acta Cryst., 19 (1965) 14-19.
- [18] N. Hakmeh, O. Merdrignac-Conanec, X-H. Zhang, Method of manufacturing a sulfide-based ceramic element, particularly for IR-optics applications, Patent pending, Application number: EP14176610.5 (2014).
- [19] J. Rodriguez-Carvajal, Recent advances in magnetic structure determination by neutron powder diffraction, Physica B: Condensed Matter, 192 (1-2) (1993) 55-69.

- [20] A. Janca, K. Tereszchuk, P.F. Bernath, N.F. Zobov, S.V. Shirin, O.L. Polyansky, J. Tennyson, Emission spectrum of hot HDO below  $4000\text{ cm}^{-1}$ , *J. Mol. Spectrosc.* 219 (2003) 132–135.
- [21] R. Lemus, Vibrational excitations in  $\text{H}_2\text{O}$  in the framework of a local model, *J. Mol. Spectrosc.* 225 (2004) 73–92.
- [22] D.A. Panayotov, J.T. Yates Jr., Depletion of conduction band electrons in  $\text{TiO}_2$  by water chemisorption - IR spectroscopic studies of the independence of Ti–OH frequencies on electron concentration, *Chemical Physics Letters*, 410 (2005) 11–17.
- [23] R.A. Nyquist, R.O. Kagel, C. Putzig, A. Leugers, *The Handbook of Infrared and Raman Spectra of Inorganic Compounds and Organic Salts*, Academic Press: San Diego, CA, (1996).
- [24] J.A. Capobianco, F. Vetrone, T. D'Alesio, G. Tessari, A. Speghini, M. Bettinelli, *Phys. Chem. Chem. Phys.* 2 (2000) 3203-3207.
- [25] N.B. Colthup, L.H. Daly, S.E. Wiberley, *Introduction to Infrared and Raman Spectroscopy*, Academic Press, 3rd Edition, chapter 9 (1990) p 319.
- [26] B.J. Tsay and L.H. Wang, A study on infrared transmission of lanthanum sulfide and oxysulfide in the 2.5-14  $\mu\text{m}$  region, *Mater. Lett.*, 34 (3-6) (1998) 180-183.
- [27] P. Besançon, Teneur en oxygène et formule exacte d'une famille de composés habituellement appelés "variété  $\beta$ " ou "phase complexe" des sulfures de terres rares, *J. Solid State Chem.*, 7 (1973) 232-240.
- [28] P. Nikolaev and I. Vasileva, Vapor pressure determination for solid and liquid  $\text{La}_2\text{S}_3$  using boiling points, *Inorganic Materials*, 44(12) (2008) 1367-1371.
- [29] A.A. Kamarzin, K.E. Mironov, V.V. Sokolov, Yu.N. Malovitsky and I.G. Vasil'yeva, Growth and properties of lanthanum and rare-earth metal sesquisulfide crystals, *J. Cryst. Growth*, 52, Part 2 (1981) 619-622.

- [30] P. Li, W. Jie and H. Li, Influences of hot-pressing conditions on the optical properties of lanthanum sulfide ceramics, *J. Amer. Ceram. Soc.* 94(4) (2011) 1162-1166.
- [31] M. Picon, L. Domange, J. Flahaut, M. Guittard, M. Patrie, Les sulfures  $\text{Me}_2\text{S}_3$  et  $\text{Me}_3\text{S}_4$  des éléments de terres rares, *CR Acad. Sci. Paris*, V 1-3 (1960) 221–228.

## Figure captions

Fig. 1. XRD patterns of raw (as-combusted) powders (La/Ca=2.7) before and after treatment under  $\text{H}_2\text{S}$  at  $1000^\circ\text{C}$  for 4 h

Fig. 2. FTIR spectra of raw powders (La/Ca=2.7) before and after treatment under  $\text{H}_2\text{S}$  at  $1000^\circ\text{C}$  for 4 h

Fig. 3. SEM images of the (a) as-combusted powder and (b) powder after sulfurization

Fig. 4. Photographs of (a) CLS1 (b) CLS2 (c) CLS3 (d) CLS5 and (e) CLS7 samples

Fig. 5. XRD patterns of the HPed CLS ceramics reported in Table 1.

Fig. 6. IR transmission spectra of transparent samples

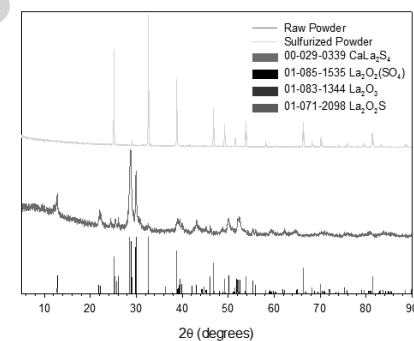


Fig. 1

Accepted manuscript

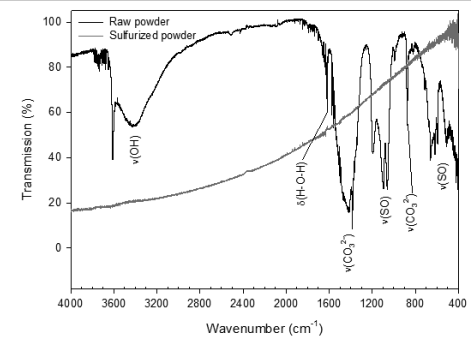


Fig. 2

Accepted manuscript

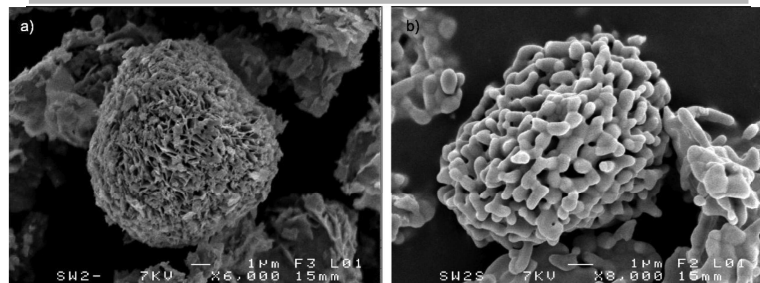


Fig. 3

Accepted manuscript

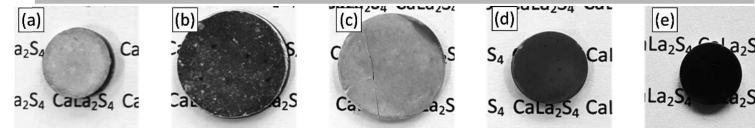


Fig. 4

Accepted manuscript

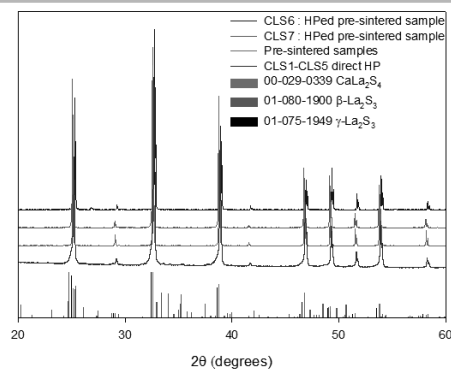


Fig. 5

Accepted manuscript

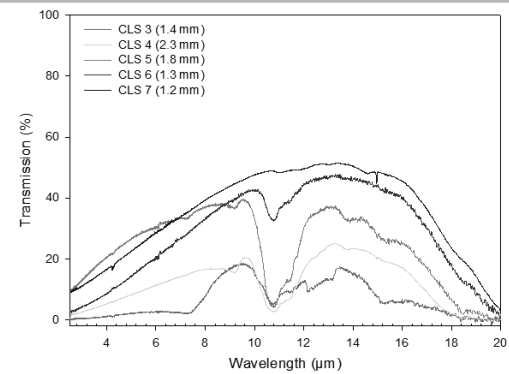


Fig. 6

Accepted manuscript